Anomalously interacting new extra vector bosons and their first LHC constraints

M. V. Chizhov

Centre for Space Research and Technologies, Faculty of Physics,
University of Sofia, 1164 Sofia, Bulgaria and
Dzhelepov Laboratory of Nuclear Problems,
Joint Institute for Nuclear Research, 141980, Dubna, Russia

V. A. Bednyakov, I. R. Boyko, J. A. Budagov, M. A. Demichev, and I. V. Yeletskikh

Dzhelepov Laboratory of Nuclear Problems,
Joint Institute for Nuclear Research, 141980, Dubna, Russia

(Dated: 14. 10. 2011)

In this review phenomenological consequences of the Standard Model extension by means of new spin-1 chiral fields with the internal quantum numbers of the electroweak Higgs doublets are summarized. The prospects for resonance production and detection of the chiral vector Z^* and $W^{*\pm}$ bosons at the LHC energies are considered on the basis of quantitative simulations within the CompHEP/CalcHEP package. The Z^* boson can be observed as a Breit-Wigner resonance peak in the invariant dilepton mass distributions in the same way as the well-known extra gauge Z' bosons. However, the Z^* bosons have unique signatures in transverse momentum, angular and pseudorapidity distributions of the final leptons, which allow one to distinguish them from other heavy neutral resonances.

In 2010, with 40 pb^{-1} of the LHC proton-proton data at the energy 7 TeV, the ATLAS detector was used to search for narrow resonances in the invariant mass spectrum of e^+e^- and $\mu^+\mu^-$ final states and high-mass charged states decaying to a charged lepton and a neutrino. No statistically significant excess above the Standard Model expectation was observed. The exclusion mass limits of 1.15 TeV/c^2 and 1.35 TeV/c^2 were obtained for the chiral neutral Z^* and charged W^* bosons, respectively. These are the first direct limits on the W^* and Z^* boson production.

Based on the above, a novel strategy for the chiral boson search in the LHC dijet data is discussed. For almost all currently considered exotic models the relevant signal is expected in the central dijet rapidity region $y_{1,2} \simeq 0$ and $|y_1 - y_2| \simeq 0$. On the contrary, the chiral bosons do not contribute to this region but produce an excess of dijet events far away from it. In particular, for these bosons the appropriate kinematical restrictions lead to a dip in the centrality ratio distribution over the dijet invariant mass instead of a bump expected in the most exotic models.

I. INTRODUCTION

Gauge interactions are the only well-established fundamental interactions in Nature. The method of the covariant derivatives leads to the unique minimal form of the gauge boson couplings to the matter fermions. Nevertheless, the Yukawa interactions of the Higgs bosons are also necessary for self-consistent construction of the Standard Model (SM). Furthermore, although the gauge symmetry allows anomalous interactions in the initial Lagrangian, all known fundamental spin-1 bosons (photon, $W^{\pm}$, Z boson and gluons) possess only renormalizable minimal interactions with the known fermions. The anomalous interactions are considered as effective ones and are generated at the level of the quantum loop corrections. They are usually proportional to the additional square of a small coupling constant and can be neglected in the first-order approximation.

New heavy neutral gauge bosons are predicted in many extensions of the SM. They are associated with additional U(1)$'$ gauge symmetries and are generically called Z' bosons. The minimal gauge interactions of these bosons with matter lead to the well-known angular distribution of outgoing leptons (the Z' decay product) in the dilepton center-of-mass reference frame

$$\frac{\mathrm{d}\sigma_{Z'}}{\mathrm{d}\cos\theta^*} \propto 1 + A_{\mathrm{FB}} \cdot \cos\theta^* + \cos^2\theta^*, \tag{1}$$

which at present is interpreted as a canonical signature for the intermediate vector (spin-1) bosons. The coefficient A_{FB} defines the backward-forward asymmetry, depending on P-parity of Z' boson couplings to matter.

In addition, another type of spin-1 bosons may exist, which leads to a different signature in the angular distribution. This follows from the presence of different types of relativistic spin-1 fermion currents $\bar{\psi}\gamma^{\mu}(1 \pm \gamma^5)\psi$ and $\partial_{\nu}[\bar{\psi}\sigma^{\mu\nu}(1 \pm \gamma^5)\psi]$, which can couple to the corresponding bosons. A clear example of such kind of interactions is provided by the hadron physics of the quark-antiquark mesons, which is considered as a low-energy QCD effective theory, where gluon and quark degrees of freedom are substituted by physical hadronic states. It was pointed out [1] that *three different* quantum numbers J^{PC} of existing neutral spin-1 mesons, 1^{--}, 1^{++} and 1^{+-}, cannot be assigned just to *two* vector $\bar{q}\gamma^{\mu}q$ and axial-vector $\bar{q}\gamma^{\mu}\gamma^5 q$ quark states, which possess quantum numbers 1^{--} and 1^{++}, respectively. The additional quark states $\partial_{\nu}(\bar{q}\sigma^{\mu\nu}q)$ and $\partial_{\nu}(\bar{q}\sigma^{\mu\nu}\gamma^5 q)$ are required, which also describe vector and axial-vector mesons, but with different transformation properties with respect to the Lorentz group and with different quantum numbers 1^{--} and 1^{+-}, respectively. This example demonstrates that the pure tensor state, b_1 meson, exists. Furthermore, due to strong dynamics, vector ρ and ρ' mesons have minimal and anomalous couplings with vector $\bar{\psi}\gamma^{\mu}\psi$ and tensor $\partial_{\nu}(\bar{\psi}\sigma^{\mu\nu}\psi)$ interpolating currents comparable in magnitude [2–5]. The both currents have the same quantum numbers $\mathrm{J}^{PC} = 1^{--}$ and mix. Since the parity and charge conjugation are conserved in QCD, they define the quantum numbers of the mesons.

The mesons assigned to the tensor quark states are some types of "excited" states as far as the only orbital angular momentum with $L = 1$ contributes to the total angular momentum, while the total spin of the system is zero. This property manifests itself in their derivative couplings to matter and a different chiral structure of the anomalous interactions in comparison with the minimal gauge ones. In contrast with the minimal gauge couplings, where either only left-handed or right-handed fermions participate in the interactions, the tensor currents mix both left-handed and right-handed fermions. Therefore, like the Higgs particles, the corresponding bosons carry a nonzero chiral charge. To our knowledge, such bosons were first introduced by Kemmer [6] and they naturally appear in the extended conformal supergravity theories [7]. In fact, this QCD feature can be realized in electroweak physics as well like the technicolor models. This analogy gives us arguments in favor of existence of anomalously interacting vector bosons.

Up to now no search for excited bosons has been done, but regular searches for the excited lepton and quark states f^* have been carried out at the modern colliders, such as LEP [8–10], HERA [11, 12] and Tevatron [13, 14]. These excited fermions have magnetic moment (Pauli) type couplings to ordinary matter

$$\mathcal{L}^{f^*}_{\text{excited}} = \frac{g}{\Lambda}\bar{f}^*\sigma^{\mu\nu}f\left(\partial_\mu Z_\nu - \partial_\nu Z_\mu\right) + \text{h.c.}, \tag{2}$$

where the parameter Λ is connected to the compositeness mass scale of the new physics. There are no objections to interpreting the interactions (2) from a different point of view, introducing excited boson states instead of fermionic ones ("shifting the $*$-sign to the right from f to Z")

$$\mathcal{L}^{Z^*}_{\text{excited}} = \frac{g}{\Lambda}\bar{f}\,\sigma^{\mu\nu}f\left(\partial_\mu Z^*_\nu - \partial_\nu Z^*_\mu\right). \tag{3}$$

This "symmetry" between excited fermions and bosons further supports our interest in consideration of the anomalously interacting vector bosons.

This review paper summarizes our attempts [15–19] to fill the gap in the consideration of experimental properties of heavy chiral bosons and continues discussions of possibilities of disentangling them from other particles.

The material below is given in the following order. In section II a simple chiral boson model is formulated for further consideration. Section III contains our numerical estimations of the boson properties within the framework of the CompHEP/CalcHEP package [20–22]. To this end a new model has been implemented, which includes additional new bosons and their corresponding interactions. In section IV the first experimental constraints on the masses of both chiral vector bosons are given. Section V briefly describes new unique signatures of the bosons in dijet final states. Our conclusions are given in section VI.

II. THE CHIRAL BOSON MODEL

Let us assume that the electroweak gauge sector of the SM is extended by a doublet of new spin-1 *chiral* bosons $\boldsymbol{W}^*_\mu$ with the internal quantum numbers of the SM Higgs boson. There are at least three different classes of theories, all motivated by the Hierarchy problem, which predict new vector weak doublets with masses not far from the electroweak scale. In particular, they can originate from the extensions of the SM such as Gauge-Higgs unification, larger gauge groups or technicolor models [23]. However, due to the lack of fully realistic models, the collider expectations for signals from these chiral bosons have not yet been studied in detail. Nevertheless, it is possible to point out several model-independent and unique signatures which allow one to identify production of such bosons at the hadron colliders [15].

Since the tensor current mixes the left-handed and right-handed fermions, which in the SM are assigned to different representations, the gauge doublet should have only anomalous interactions

$$\mathcal{L}^* = \frac{g}{M}\left(\partial_\mu W^{*-}_\nu \;\partial_\mu \overline{W}^{*0}_\nu\right)\cdot\overline{D_R}\,\sigma^{\mu\nu}\begin{pmatrix}U_L\\ D_L\end{pmatrix} + \frac{g}{M}\left(\overline{U_L}\;\overline{D_L}\right)\sigma^{\mu\nu}D_R\cdot\begin{pmatrix}\partial_\mu W^{*+}_\nu\\ \partial_\mu W^{*0}_\nu\end{pmatrix}, \qquad (4)$$

where M is the boson mass, g is the coupling constant of the $\mathrm{SU(2)_W}$ weak gauge group, and U and D generically denote up-type and down-type leptons and quarks. This choice of couplings makes identical all partial fermionic decay widths of the well-known hypothetical W' boson with the SM-like interactions

$$\mathcal{L}'_{CC} = \frac{g}{\sqrt{2}}\,W'^-_\mu\cdot\overline{D_L}\gamma^\mu U_L + \frac{g}{\sqrt{2}}\,\overline{U_L}\gamma^\mu D_L\cdot W'^+_\mu \qquad (5)$$

and the charged $W^{*\pm}$ boson with the same mass. Here we also assume universality of lepton and quark couplings with different flavors. In full analogy with the above-mentioned mesons these bosons, coupled to the tensor quark currents, can be considered as *excited* states. This property manifests itself in their derivative couplings to fermions and in the different chiral structure of the interactions in contrast to the minimal gauge interactions.

For simplicity, in (4) we have introduced only interactions with the down-type right-handed singlets, D_R. In particular, in order to allow a possibility of detecting the neutral CP-even $Z^* = (W^{*0} + \overline{W}^{*0})/\sqrt{2}$ bosons via their decays into charged leptons (the Drell–Yan-like process) they should couple to the *down* type of fermions

$$\mathcal{L}^*_{NC} = \frac{g}{2\sqrt{2}M}\left(\bar\ell\sigma^{\mu\nu}\ell + \bar d\sigma^{\mu\nu}d\right)\left(\partial_\mu Z^*_\nu - \partial_\nu Z^*_\mu\right). \qquad (6)$$

Since we have introduced the complex $\boldsymbol{W}^*_\mu$ doublet, there is an additional neutral CP-odd $\tilde{Z}^* = (W^{*0} - \overline{W}^{*0})/\sqrt{2}$ boson. However, in the case of light final states it is impossible to

discriminate the multiplicative quantum numbers of the neutral bosons, namely P and C. Therefore, in the following calculations we will consider only one of them, for instance, the Z^* boson.

For comparison we will consider topologically analogous gauge interactions of the Z' boson

$$\mathcal{L}'_{NC} = \frac{g}{2}\left(\bar{\ell}\gamma^\mu\ell + \bar{d}\gamma^\mu d\right) Z'_\mu \tag{7}$$

with the same mass M. The coupling constants are chosen in such a way that all fermionic decay widths in the Born approximation of the both neutral bosons are identical. It means that their total production cross sections at the hadron colliders are nearly equal up to next-to-leading order corrections. Their total fermionic decay width

$$\Gamma = \frac{g^2}{4\pi} M \approx 0.034\ M \tag{8}$$

is sufficiently narrow so that they can be identified as resonances at the hadron colliders in the Drell–Yan process.

Furthermore, as several Higgs doublets are introduced in many of the SM extensions, the realistic model could include several gauge doublets. Using the charge-conjugated doublet

$$\boldsymbol{W}^{*\,\mathrm{c}}_\mu = \begin{pmatrix} \overline{W}^{*0}_\mu \\ -W^{*-}_\mu \end{pmatrix} \tag{9}$$

(or new ones with the hypercharges opposite to the $\boldsymbol{W}^*_\mu$ doublet) one can construct more complicated models including up-type right-handed singlets, U_R, as well.

III. NUMERICAL SIMULATIONS OF THE CHIRAL BOSONS

Up to now, any excess in the yield of the Drell–Yan process with high-energy invariant mass of the lepton pairs remains the clearest indication of possibile production of a new heavy neutral boson at the hadron colliders. Therefore, we will first concentrate on consideration of the production and decay of neutral bosons, where full kinematics is experimentally reconstructible. In what follows we will use the CompHEP/CalcHEP package [20–22] for the numerical calculations of various distributions for the inclusive processes $pp \to \gamma/Z/Z' + X \to \ell^+\ell^- + X$ and $pp \to \gamma/Z/Z^* + X \to \ell^+\ell^- + X$ with a CTEQ6M choice for the proton parton distribution set at $\sqrt{s} = 10$ TeV. For both final leptons we impose angular restrictions (cuts) on the pseudorapidity range $|\eta_\ell| < 2.5$ and the transverse momentum $p_\mathrm{T} > 20$ GeV/c, which are relevant to the general LHC detectors.

Let us choose $M = 1$ TeV/c^2 as a reference mass for new heavy bosons. For the high dilepton masses the cross sections of the new boson production with this mass at the peak is about two orders of magnitude higher (in our model) than the corresponding Drell–Yan

background, being the SM γ and Z boson tails in the invariant dilepton mass distributions (Fig. 1, left). Therefore, the peak(s) should be clearly visible.

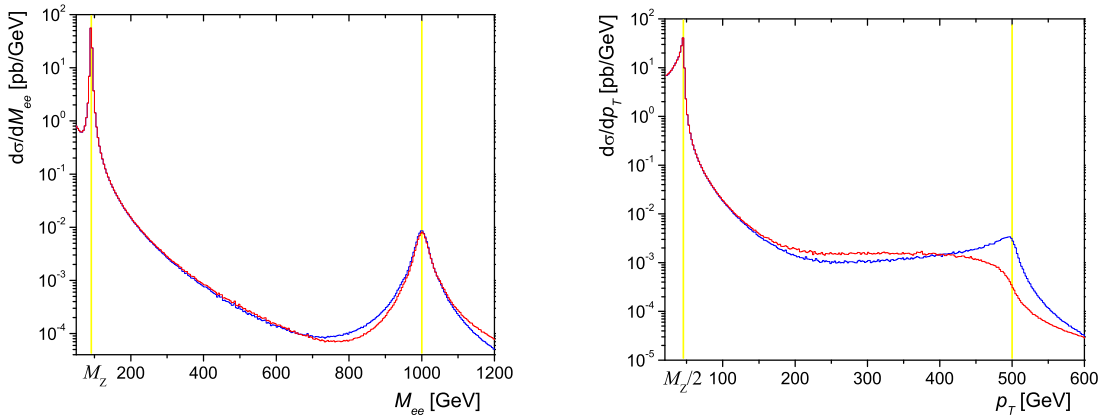

FIG. 1: The invariant dilepton mass distributions (left) for the Z' boson (blue) and the excited chiral Z^* boson (red) with mass 1 TeV/c^2 together with the Drell–Yan SM background (from the photon and the Z boson) at the LHC for $\sqrt{s} = 10$ TeV. The differential cross-sections (right) for the gauge Z' boson (blue) and the excited chiral Z^* boson (red) with the Drell–Yan SM background as functions of the lepton transverse momentum at the CERN LHC.

The peaks in the dilepton invariant mass distributions originate from the Breit–Wigner propagator form, which is *the same* for both the gauge and chiral *neutral* bosons in the Born approximation.

Concerning discovery of the *charged* heavy boson at the hadron colliders one believes that the cleanest method is detection of its subsequent leptonic decay into an isolated high transverse-momentum charged lepton (better without a prominent associated jet activity). In this case the heavy new boson can be observed through the Jacobian peak in the transverse $p_{\rm T}$ or $m_{\rm T}$ distribution. It has become proverbial (see, for example, the textbook [24]) that the Jacobian peak is an inevitable characteristic of any two-body decay. However, it is not the case for decays of the new chiral bosons [25]. It has been found in [26] that tensor interactions lead to a new angular distribution of the outgoing fermions

$$\frac{{\rm d}\sigma(q\bar{q} \to Z^*/W^* \to f\bar{f})}{{\rm d}\cos\theta} \propto \cos^2\theta, \tag{10}$$

in comparison with the well-known vector interaction result

$$\frac{{\rm d}\sigma(q\bar{q} \to Z'/W' \to f\bar{f})}{{\rm d}\cos\theta} \propto 1 + \cos^2\theta\,. \tag{11}$$

It was realized later [25] that this property ensures a distinctive signature for the detection of the new interactions at the hadron colliders. At first sight, the small difference between

the distributions (10) and (11) seems unimportant. However, the absence of the constant term in the first case results in very new experimental signatures.

The angular distribution for vector interactions (11) includes a nonzero constant term, which leads to the kinematical singularity in the $p_{\rm T}$ distribution of the final fermion

$$\frac{1}{\cos\theta} \propto \frac{1}{\sqrt{(M/2)^2 - p_T^2}} \tag{12}$$

in the narrow width approximation $\Gamma \ll M$

$$\frac{1}{(s-M^2)^2 + M^2\Gamma^2} \approx \frac{\pi}{M\Gamma}\delta(s-M^2). \tag{13}$$

This singularity is transformed into a well-known Jacobian peak due to a finite width of the resonance. In contrast, the pole in the decay distribution of the Z^*/W^* bosons is canceled out and the fermion transverse momentum $p_{\rm T}$ distribution even reaches zero at the kinematical endpoint $p_{\rm T} = M/2$, rather than the Jacobian peak (at the kinematical endpoint $M/2$) for the gauge bosons (Fig. 1, right). Therefore, even the lepton transverse momentum distribution demonstrates a difference between the gauge and chiral bosons.

According to (10), there exists a characteristic plane, perpendicular to the beam axis in the parton rest frame, where emission of final-state pairs is forbidden. The nonzero probability in the perpendicular direction in the laboratory frame is due to the longitudinal boosts of colliding partons. So, at the Fermilab Tevatron the production of such heavy bosons occurs almost at the threshold with approximately zero longitudinal momenta. Hence, the lepton pseudorapidity distribution for the chiral bosons has a minimum at $\eta_\ell = 0$ (Fig. 2, left). On the other hand, the CERN LHC is sufficiently powerful to produce heavy bosons with the mass $M = 1$ TeV/c^2 with high longitudinal boosts. Therefore, the pseudorapidity distributions for the gauge and chiral bosons at the LHC look similar (Fig. 2, right).

In order to make more substantial and experiment-looking conclusions, let us investigate signal distributions selecting only "on-peak" events with the invariant dilepton masses in the range 800 GeV/c^2 $< M_{\ell\ell} <$ 1200 GeV/c^2. To this end (as a test example) in [17] for these dilepton masses and kinematical restrictions $|\eta_\ell| < 2.5$ and the transverse lepton momentum $p_{\rm T} > 20$ GeV/c we have simulated production of dilepton events via $pp \to \gamma/Z/Z' + X \to \ell^+\ell^- + X$ and $pp \to \gamma/Z/Z^* + X \to \ell^+\ell^- + X$ for the LHC integrated luminosity of 100 pb^{-1} and $\sqrt{s} = 10$ TeV. As far as the center-of-mass energy for the 2010–2011 runs was 7 TeV, at which the cross sections are roughly half as large, 200 pb^{-1} of data will be equivalent to the case with $\sqrt{s} = 10$ TeV. For the Z' and Z^* bosons (with mass 1 TeV/c^2) production cross-sections $\sigma_{Z'} = 0.45$ pb and $\sigma_{Z^*} = 0.41$ pb were obtained. The values respectively transform into 44.9 and 41.2 dilepton events in the mass window of 800 GeV/c^2 $< M_{\ell\ell} <$ 1200 GeV/c^2 (see Fig. 3). Under the same kinematical conditions the SM gives 0.6 events with the production cross-section 5.75 fb.

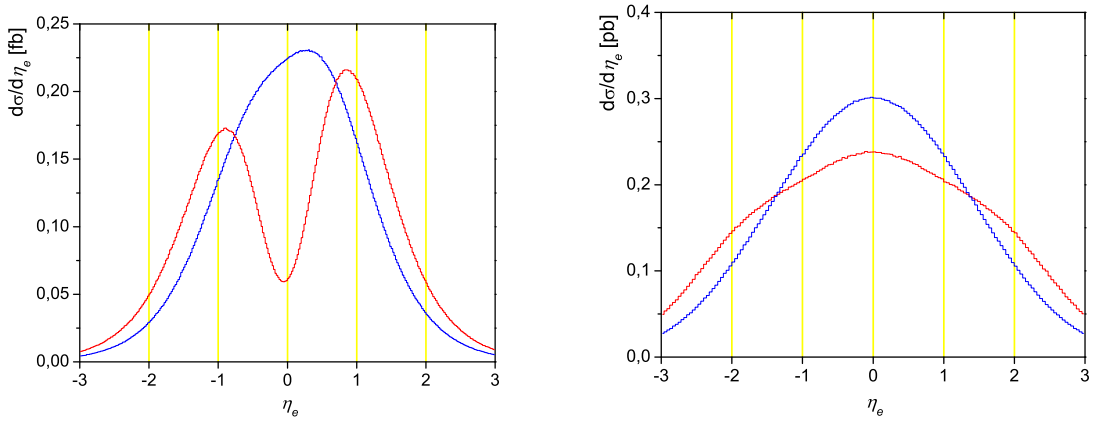

FIG. 2: The differential cross sections for the gauge Z' boson (blue) and the excited chiral Z^* boson (red) decaying to a lepton pair with the invariant mass 800 GeV/c^2 < $M_{\ell\ell}$ < 1200 GeV/c^2 as functions of the lepton pseudorapidity at the Fermilab Tevatron $\sqrt{s} = 1.96$ TeV (left) and at the CERN LHC $\sqrt{s} = 14$ TeV (right).

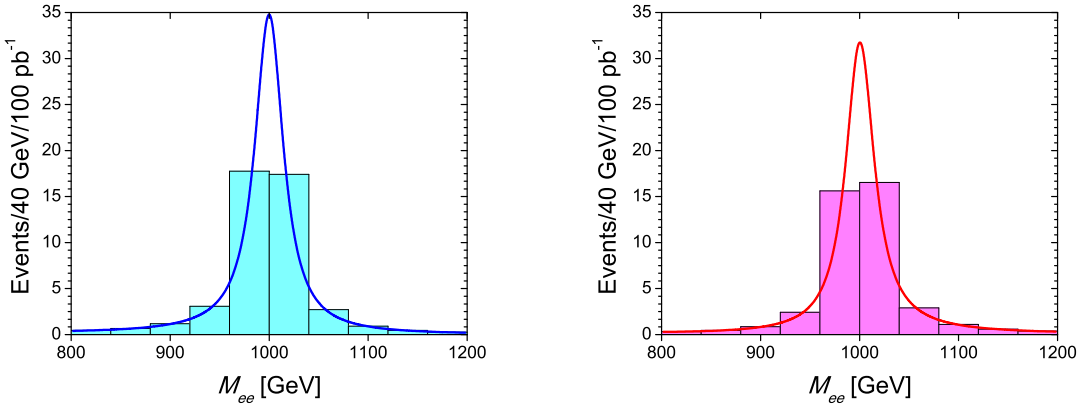

FIG. 3: The invariant mass dilepton distributions for the gauge Z' boson (left) and the excited chiral Z^* boson (right) simulated with the common mass 1 TeV/c^2. They consist of 44.9 and 41.2 dilepton events in the mass window of 800 GeV/c^2 < $M_{\ell\ell}$ < 1200 GeV/c^2 for Z' and Z^* bosons.

As already mentioned, the peaks in the invariant mass distributions originate from the Breit–Wigner propagator form, which is the same for both Z' and Z^* bosons in the leading Born approximation. Therefore, in order to discriminate them we need to investigate additional distributions selecting only "on-peak" events with the invariant dilepton masses in the optimal window size $[M - 2\Gamma, M + 2\Gamma]$. According to [15], a crucial difference between the neutral chiral bosons and other resonances should come from the analysis of the angular distribution of the final-state leptons with respect to the boost direction of the heavy boson in the rest frame of the latter (the Collins–Soper frame [27]) (Fig. 4). Instead of a smoother angular distribution for the gauge interactions (left), a

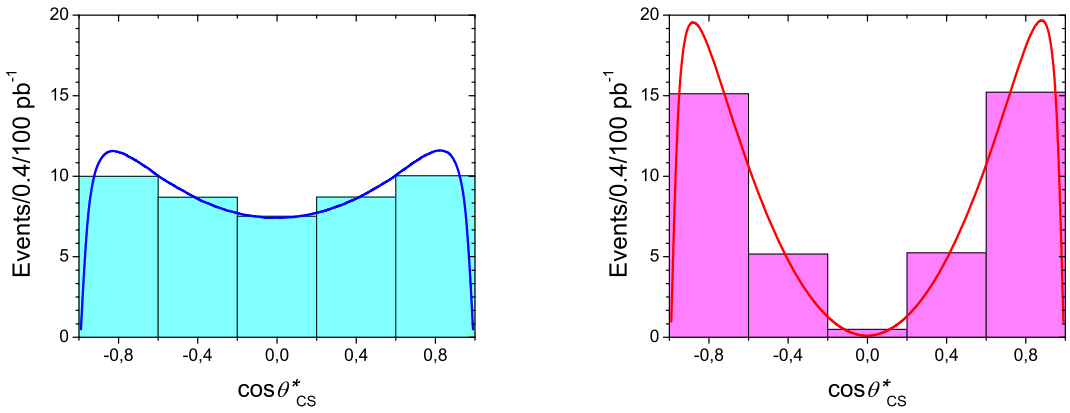

FIG. 4: The differential lepton angular distributions of the gauge Z' boson (left) and the excited chiral Z^* boson (right) as functions of $\cos\theta^*_{\rm CS}$ for $M = 1$ TeV/c^2.

peculiar "swallowtail" shape of the chiral boson distribution (right) occurs with a dip at $\cos\theta^*_{\rm CS} = 0$. It will indicate the presence of the new interactions. Neither scalars nor other particles possess such a type of angular behavior. Indeed, the angular distribution of outgoing leptons for the Z^* bosons will lead to the large negative value of the so-called centre-edge asymmetry $A_{\rm CE}$:

$$\sigma \times A_{\rm CE} = \int_{-\frac{1}{2}}^{+\frac{1}{2}} \frac{{\rm d}\sigma}{{\rm d}\cos\theta^*_{\rm CS}}\,{\rm d}\cos\theta^*_{\rm CS} - \left[\int_{+\frac{1}{2}}^{+1} \frac{{\rm d}\sigma}{{\rm d}\cos\theta^*_{\rm CS}}\,{\rm d}\cos\theta^*_{\rm CS} + \int_{-1}^{-\frac{1}{2}} \frac{{\rm d}\sigma}{{\rm d}\cos\theta^*_{\rm CS}}\,{\rm d}\cos\theta^*_{\rm CS}\right], \quad (14)$$

while the distributions of other known resonances (even with different spins) possess

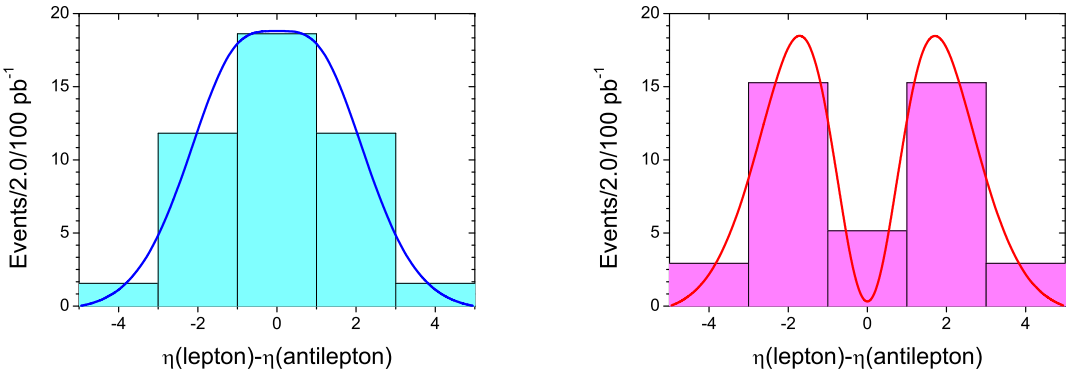

FIG. 5: The differential distributions for the gauge Z' boson (left) and the excited chiral Z^* boson (right) as functions of the difference of the lepton pseudorapidities for $M = 1$ TeV/c^2.

positive or near-zero asymmetries. Using this asymmetry, one can strongly reduce the systematic uncertainties from the hadron structure [28].

Another "unexpected" consequence of the new form of angular distribution (10) is a very different shape of the event distribution over pseudorapidity difference $(\eta_1 - \eta_2)$ between both outgoing charged leptons. It is shown in Fig. 5. Combining these distributions one will have a possibility of differentiating these bosons for higher resonance masses.

We would like again to consider the distributions of the lepton transverse momentum $p_{\rm T}$. As mentioned before and demonstrated for our simulated sample in Fig. 6, the relevant

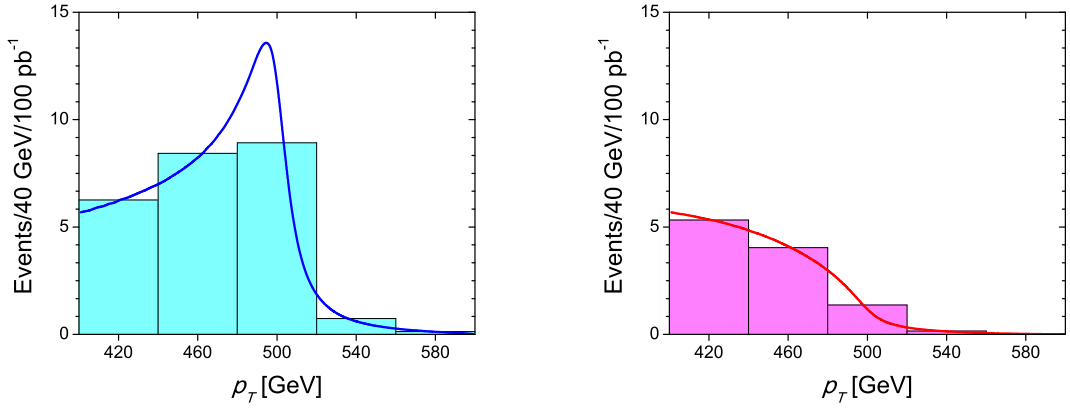

FIG. 6: The differential distributions for the Z' boson (left) and the chiral excited Z^* boson (right) as functions of the lepton transverse momentum $p_{\rm T}$ for $M = 1$ TeV/c^2 the LHC integrated luminosity of 100 pb^{-1} and $\sqrt{s} = 10$ TeV.

Z^* and W^* boson decay distributions have a broad smooth hump with the maximum below the kinematical endpoint, instead of an "expected" sharp Jacobian peak. Therefore, in contrast to the usual procedure of the direct and precise determination of the W' resonance mass, the new distribution does not allow doing it for W^* bosons. Moreover, even a relatively small decay width of the chiral bosons has a wide $p_{\rm T}$ distribution that obscures their identification as resonances at hadron colliders.

IV. THE FIRST EXPERIMENTAL CONSTRAINTS ON THE CHIRAL BOSONS

The first direct experimental search for the excited chiral vector bosons was performed by the ATLAS collaboration [29–31] in 2010. At the LHC energy of 7 TeV with the integral luminosity around 40 pb^{-1} the ATLAS detector was used for searching for narrow resonances in the invariant mass spectrum above 110 GeV/c^2 of e^+e^- and $\mu^+\mu^-$ final states. The main physical results of the relevant paper "Search for high mass dilepton resonances in pp collisions at $\sqrt{s} = 7$ TeV with the ATLAS experiment" [32] are presented in Fig. 7 together with main backgrounds and expected Z' decay signals for three masses

around 1 TeV/c^2. Expected signals from the Z^* boson decays considered in this paper (are shown in Fig. 8) have similar shapes and approximately 40% larger cross sections. Three "interesting" events in the vicinity of $m_{ee} = 600$ GeV/c^2 and a single event at $m_{\mu\mu} = 768$ GeV/c^2 are observed. All details of the data selection and the physical data analysis can be found in [32]. It is seen that both the dielectron and dimuon invariant

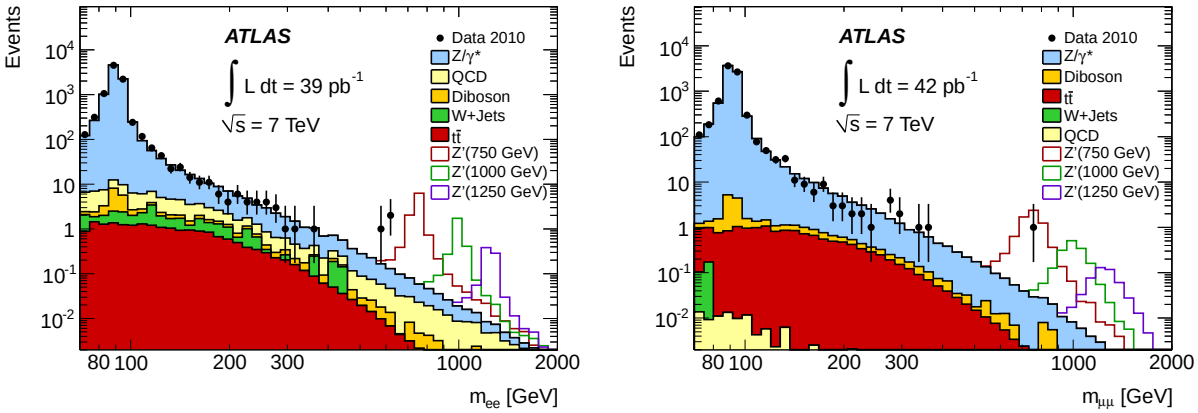

FIG. 7: Dielectron (left) and dimuon (right) invariant mass distribution measured by the ATLAS collaboration in 2010 [32]. They are compared with all expected backgrounds and three example Z' signals.

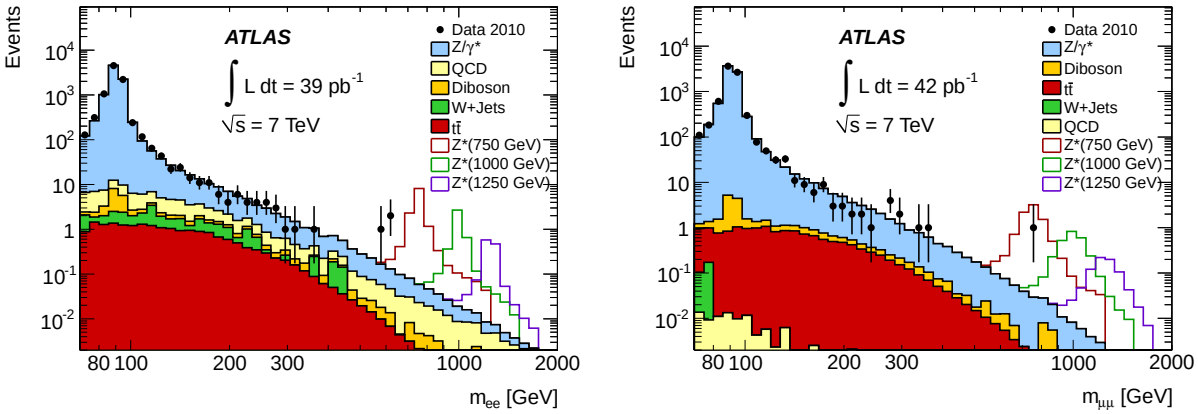

FIG. 8: Dielectron (left) and dimuon (right) invariant mass distribution after final selection, compared to the stacked sum of all expected backgrounds, with three example Z^* signals overlaid.

mass distributions are well described by the prediction from SM processes. From these figures one can conclude that no statistically significant excess above the SM expectation is observed with these data samples. Nevertheless, these distributions were for the first time used to obtaine a lower direct mass limit (1.152 TeV/c^2, see below) for the neutral

chiral Z^* boson described in this paper. To this end, 95% C.L. exclusion limits on Z^* production and its dilepton decay, σB, for the combination of the electron and muon Z^* boson decay channels were used. The combination was performed by defining the likelihood function in terms of the total number of Z^* events produced in both channels.

In the three cases (dielectron, dimuon and combined channels), the 95% C.L. σB limit was used to set mass limits for each of the considered models. The observed combined mass limit for the Sequential Standard Model $Z'_{\rm SSM}$ is 1.048 TeV/c^2. The limits on the E6-motivated Z' bosons are in the range 0.738–0.900 TeV/c^2. Although the angular lepton decay distributions are not the same for Z' and Z^* bosons, it was found that the difference in geometrical acceptance is negligible for the boson pole masses above 750 GeV/c^2. Therefore, the same procedure as for the Z' bosons is used to calculate the limit on $\sigma B(Z^* \to \ell^+\ell^-)$ and on the Z^* boson mass in each channel and for their combination. Finally the observed combined lower mass limit for the Z^* boson is 1.152 TeV/c^2. This is the first direct mass limit on this particle. The Z^* limits are about 100–200 GeV/c^2 more stringent than the corresponding limits on all considered Z' bosons.

Furthermore, in 2010 the ATLAS collaboration searched for high-mass states, such as heavy charged gauge bosons (W', W^*), decaying to a charged lepton and a neutrino (see Fig. 9). The relevant paper "Search for high-mass states with one lepton plus missing transverse momentum in proton-proton collisions at $\sqrt{s} = 7$ TeV with the ATLAS detector" contains all details of event selection and physical data analysis [33].

The search for heavy charged resonances inclusively produced at the LHC looks more complicated than the search for neutral states due to the absence of the second decay particle — the undetectable neutrino. In this case the kinematic variable used to identify the W'/W^* is the transverse mass

$$m_{\rm T} = \sqrt{2 p_{\rm T} E_{\rm T}^{\rm miss} (1 - \cos\phi_{l\nu})}$$

which displays a Jacobian peak that, for $W' \to \ell\nu$, falls sharply above the resonance mass. Here $p_{\rm T}$ is the lepton transverse momentum, $E_{\rm T}^{\rm miss}$ is the magnitude of the missing transverse momentum (missing $E_{\rm T}$), and $\phi_{l\nu}$ is the angle between the $p_{\rm T}$ and missing $E_{\rm T}$ vectors. In the analysis [33], "transverse" refers to the plane perpendicular to the colliding beams, "longitudinal" means parallel to the beams, θ and ϕ are the polar and azimuthal angles with respect to the longitudinal direction, and pseudorapidity is defined as $\eta = -\ln(\tan(\theta/2))$.

The main physical results obtained in [33] and relevant to our consideration are given in Fig. 9. The left panel of Fig. 9 shows the $p_{\rm T}$, missing $E_{\rm T}$, and $m_{\rm T}$ spectra measured in the muon decay channel for the data, for the expected background, and for three examples of W' signals at different masses as open histograms. The W^* boson signals are not shown. The QCD background is estimated from the data. The signal and other background samples are normalized using the integrated luminosity of the data and the

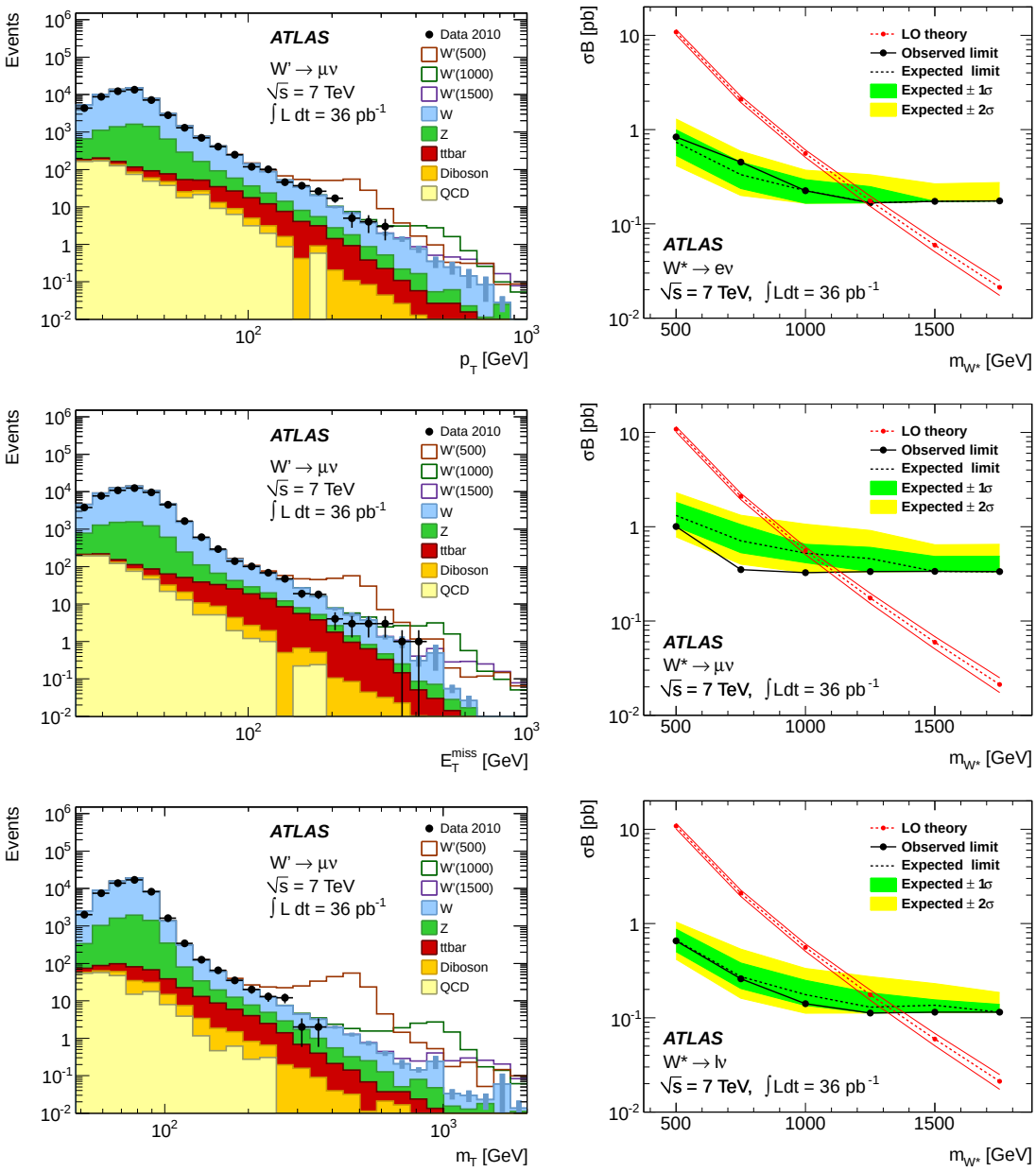

FIG. 9: Spectra of p_{T} (top), missing E_{T} (center) and m_{T} (bottom) for the muon channel (left) obtained in [33]. The points represent the ATLAS data and the filled histograms show the stacked backgrounds. Open histograms are W' signals. The QCD background is estimated from the data. Limits at 95% C.L. for W^* (right) production in the decay channels $W'/W^* \to e\nu$ (top), $W'/W^* \to \mu\nu$ (center), and their combination (bottom). The solid lines show the observed limits with all uncertainties. The expected limit is indicated with dashed lines surrounded by shaded 1σ and 2σ bands. Dashed lines show the theory predictions with their uncertainties indicated by solid lines.

NNLO (near-NNLO for t-tbar) cross sections. Furthermore, the σB uncertainties for the W' boson are obtained by varying renormalization and factorization scales and by varying PDFs. Only the latter are employed for the W^* boson search.

One can see from the figures that the agreement between the data and the expected background is rather good. No excess beyond the Standard Model expectations is observed. The lower mass limits expected and obtained from these measurements are depicted in the right panel of Fig. 9. The figure also shows the expected limits and the theoretical W'/W^* σB as a function of $m_{\rm T}$ for both channels and their combination. The intersection between the central theoretical prediction and the observed limits provides the 95% C.L. lower limit on the mass. It was found that the charged chiral W^* boson considered in the paper was excluded for masses below 1.350 TeV/c^2. These are the first direct limits on the W^* boson production.

V. DIJET SIGNALS OF THE CHIRAL BOSONS

In what follows we will extend the set of possible experimental observables of the chiral bosons to the rich field of hadron final states, in particular we consider peculiarity of the decay of these bosons into two hadronic jets. In fact we will draw extra attention to a novel signal of new physics in the dijet data at the hadron colliders. It is usually accepted that all exotic models predict that these two jets populate the central (pseudo)rapidity region where $y_{1,2} \simeq 0$. Contrariwise, the excited bosons do not contribute into this region, but produce an excess of dijet events over the almost flat QCD background in $\chi = \exp|y_1 - y_2|$ away from this region.

At the hadron colliders, inclusive dijet production has one of the largest cross sections and allows data-driven background estimation at the early stage of the collider operation. The feature can be used to search for a signal of new physics in the very early data. In particular, a possible bump in the dijet invariant mass spectrum would indicate the presence of a resonance decaying into two energetic partons. Nevertheless, we could say nothing about its nature, because this bump stems from the Breit–Wigner propagator form, which is characteristic of any type of resonance regardless of its other properties, like spin, internal quantum number, etc. Therefore, other observables are necessary in order to confirm the bump and to reveal the resonance properties.

As in the lepton case (discussed above), this kind of observable could be the dijet distribution over the polar angle θ, which is an angle between the axis of the jet pair and the beam direction in the dijet rest frame. This distribution is directly sensitive to the resonance spin and the dynamics of the underlying process [27].

While the QCD processes are dominated by t-channel gluon exchanges, which lead to the Rutherford-like dijet distribution $1/(1-\cos\theta)^2$, exotic physics processes proceed mainly through the s-channel, where the spin of the resonance uniquely defines the angular

distribution. For high-mass resonances and practically massless partons it is convenient to use the helicity formalism since the helicity is a good quantum number for massless particles.

In fact, in the center-of-momentum frame of a particle with spin s and helicity λ ($-s \leq \lambda \leq s$) decaying into two massless particles with helicities λ_1 and λ_2 the angular distribution of the outgoing particle can be written as [34]

$$\frac{\mathrm{d}\Gamma_s}{\mathrm{d}\cos\theta\,\mathrm{d}\phi} = \frac{1}{64\pi^2 M}\left|\sqrt{\frac{2s+1}{4\pi}}\,e^{i(\lambda-\delta)\phi}\,d^s_{\lambda\delta}(\theta)\,\mathcal{M}^s_{\lambda_1\lambda_2}\right|^2, \tag{15}$$

where $\delta \equiv \lambda_1 - \lambda_2$ with $-s \leq \delta \leq s$. The reduced decay amplitude $\mathcal{M}^s_{\lambda_1\lambda_2}$ is only a function of s and the helicities of the outgoing particles. It does not dependent on the azimuthal ϕ and polar θ angles. The θ dependence is concentrated only in the well-known d-functions $d^s_{\lambda\delta}(\theta)$. Furthermore, the absolute value of the dijet rapidity difference is related to the polar scattering angle θ with respect to the beam axis by the formula $\Delta y \equiv |y_1 - y_2| = \ln[(1+|\cos\theta|)/(1-|\cos\theta|)] \geq 0$ and is invariant under boosts along the beam direction. The choice of the other variable $\chi \equiv \exp(\Delta y) = (1+|\cos\theta|)/(1-|\cos\theta|) \geq 1$ is motivated by the fact that the distribution of the Rutherford scattering is flat in this variable. These variables allow systematic consideration of angular decay distributions of resonances with different spins and different interactions with partons.

The simplest case of the resonance production of a (pseudo)scalar particle h with spin 0 in the s-channel leads to a uniform decay distribution in the scattering angle

$$\frac{\mathrm{d}\Gamma_0(h \to q\bar{q})}{\mathrm{d}\cos\theta} \propto |d^0_{00}|^2 \sim 1. \tag{16}$$

The spin-1/2 fermion resonance, like an excited quark q^*, leads to asymmetric decay distributions for the given spin parton configurations

$$\frac{\mathrm{d}\Gamma_{1/2}(q^* \to qg)}{\mathrm{d}\cos\theta} \propto |d^{1/2}_{1/2,\pm1/2}|^2 \sim 1 \pm \cos\theta. \tag{17}$$

However, the choice of the variables which depend on the absolute value of $\cos\theta$ cancels out the apparent dependence on $\cos\theta$. In other words, both distributions (17) for dijet events look like uniform distributions in Δy and χ According to the simple formula

$$\frac{\mathrm{d}\Gamma}{\mathrm{d}(\Delta y/\chi)} = \frac{\mathrm{d}\cos\theta}{\mathrm{d}(\Delta y/\chi)}\,\frac{\mathrm{d}\Gamma}{\mathrm{d}\cos\theta}\,, \tag{18}$$

the uniform distribution leads to kinematical peaks at the small values $\Delta y = 0$ (the dotted curve in the left panel of Fig. 10) and $\chi = 1$ (the dotted curve in the right panel of Fig. 10)

$$\frac{\mathrm{d}\Gamma_0}{\mathrm{d}\Delta y} \propto \frac{\mathrm{e}^{\Delta y}}{(\mathrm{e}^{\Delta y}+1)^2} \qquad \text{and} \qquad \frac{\mathrm{d}\Gamma_0}{\mathrm{d}\chi} \propto \frac{1}{(\chi+1)^2}. \tag{19}$$

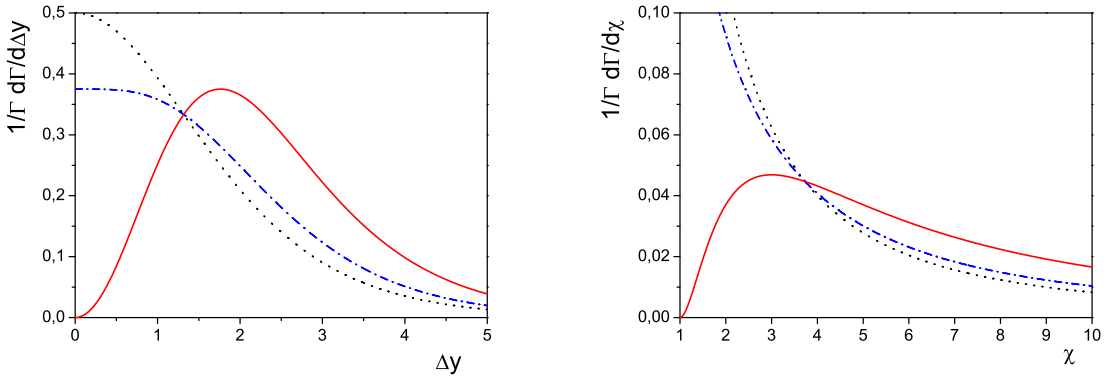

FIG. 10: The normalized angular dijet distributions as functions of the absolute value of the rapidity difference (left) and the χ variable (right) for the scalar (or/and spin-1/2) bosons, the gauge bosons with the minimal coupling and the excited bosons are shown by the dotted, dash-dotted and solid curves, respectively. From [18].

There are two different possibilities for spin-1 resonances. The gauge bosons, which are associated with additional $U(1)'$ gauge symmetry (or transform under the adjoint representation of the extra gauge group), are generally called $Z'(\boldsymbol{W}')$ particles. They have minimal gauge interactions with the known light fermions (see eqs. (7) and (5)), which preserve the fermion chiralities and possess maximal helicities $\lambda = \pm 1$. At a symmetric pp collider, like the LHC, such interactions lead to the symmetric angular distribution (11) of the decay products over the polar angle θ:

$$\frac{\mathrm{d}\Gamma_1(Z' \to q\bar{q})}{\mathrm{d}\cos\theta} \propto |d^1_{11}|^2 + |d^1_{-11}|^2 \sim 1 + \cos^2\theta\,. \tag{20}$$

Similar to the uniform distribution (16), this one also leads to kinematical peaks at small values of $\Delta y = 0$ (the dash-dotted curve in the left panel of Fig. 10) and $\chi = 1$ (the dash-dotted curve in the right panel of Fig. 10)

$$\frac{\mathrm{d}\Gamma'_1}{\mathrm{d}\Delta y} \propto \frac{\mathrm{e}^{\Delta y}(\mathrm{e}^{2\Delta y}+1)}{(\mathrm{e}^{\Delta y}+1)^4} \qquad \text{and} \qquad \frac{\mathrm{d}\Gamma'_1}{\mathrm{d}\chi} \propto \frac{\chi^2+1}{(\chi+1)^4}. \tag{21}$$

Another possibility is the resonance production and decay of new longitudinal spin-1 bosons with helicity $\lambda = 0$. These bosons arise in many extensions [23] of SM which solve the Hierarchy problem. They are transformed as doublets (Z^* W^*) under the fundamental representation of the SM $SU(2)_W$ group like the SM Higgs boson. They are above-mentioned extra chiral bosons (see (4)). While the Z' bosons with helicities $\lambda = \pm 1$ are produced in left(right)-handed quark and right(left)-handed antiquark fusion, the longitudinal Z^* bosons can be produced through the anomalous chiral couplings with

the ordinary light fermions in left-handed or right-handed quark-antiquark fusion [15]. As already noted before, these anomalous couplings lead to a different angular distribution of the resonance decay

$$\frac{\mathrm{d}\Gamma_1^*(Z^* \to q\bar{q})}{\mathrm{d}\cos\theta} \propto |d_{00}^1|^2 \sim \cos^2\theta. \tag{22}$$

As has already been noted for the dilepton case the absence of the constant term in (22) results in novel experimental signatures. First of all, the uniform distribution (16) for scalar and spin-1/2 particles and the distribution (20) for gauge vector bosons with minimal coupling include a nonzero constant term, which leads to a kinematic singularity in the transverse momentum distribution of the final parton (as for charged leptons, see (12) and (13)). After smearing of the resonance finite width the singularity is transformed into the well-known Jacobian peak (the dash-dotted curve in the left panel of Fig. 11). The analytic expression of the p_{T} distribution describing the Jacobian peak with finite width can be found in [35]. Using the same method one can derive an analogous distribution for the excited bosons (the solid curve in the left panel of Fig. 11).

$$\frac{\mathrm{d}\Gamma_1^*}{\mathrm{d}p_{\mathrm{T}}} \propto p_{\mathrm{T}}\sqrt{\sqrt{\left(4p_{\mathrm{T}}^2 - M^2\right)^2 + \Gamma^2 M^2} - 4p_{\mathrm{T}}^2 + M^2}. \tag{23}$$

In contrast to the previous case, the pole in the decay distribution of the excited bosons is canceled out and the final parton p_{T} distribution has a broad smooth hump [25] with a maximum at $p_{\mathrm{T}} = \sqrt{(M^2+\Gamma^2)/8} \simeq M/\sqrt{8}$ below the kinematic endpoint $p_{\mathrm{T}} = M/2$ instead of a sharp Jacobian peak, which obscures their experimental identification as resonances. Therefore, the transverse jet momentum is not the appropriate variable for the excited boson search.

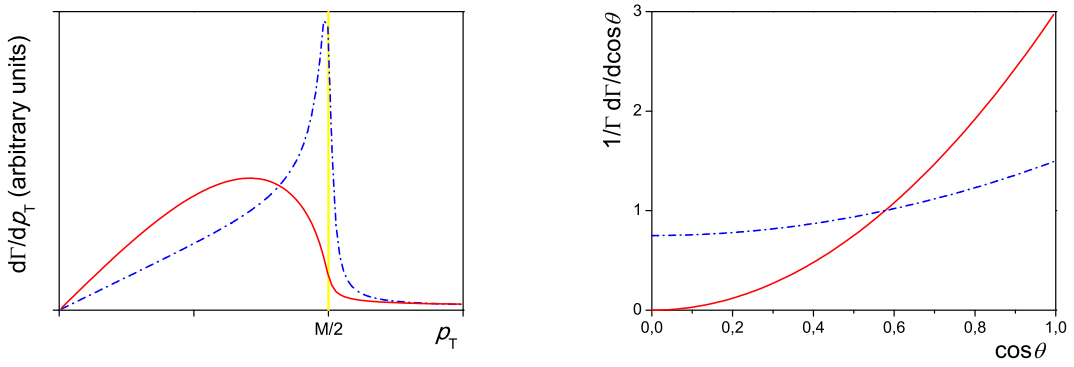

FIG. 11: The final parton transverse momentum (left) and the angular (right) distributions from the decay of the gauge (dash-dotted curves) and excited (solid curves) bosons. From [18].

Another striking feature of the distribution (22) is the forbidden decay direction perpendicular to the boost of the excited boson in the rest frame of the latter (the Collins–Soper frame [27]). It leads to a profound dip at $\cos\theta = 0$ in the Collins–Soper frame [15]

in comparison with the gauge boson distribution (the right panel in Fig. 11). Similar dips also occur at the small values $\Delta y = 0$ [17] (the solid curve in the left panel of Fig. 10) and $\chi = 1$ (the solid curve in the right panel of Fig. 10)

$$\frac{\mathrm{d}\Gamma_1^*}{\mathrm{d}\Delta y} \propto \frac{\mathrm{e}^{\Delta y}(\mathrm{e}^{\Delta y}-1)^2}{(\mathrm{e}^{\Delta y}+1)^4} \qquad \text{and} \qquad \frac{\mathrm{d}\Gamma_1^*}{\mathrm{d}\chi} \propto \frac{(\chi-1)^2}{(\chi+1)^4}. \tag{24}$$

It can be seen from Fig. 10 that the excited bosons have a unique signature in the angular distributions. They manifest themselves through the absolute minima at the small values $\Delta y = 0$ and $\chi = 1$ and absolute maxima right away from the origin. So, the rapidity difference distribution reaches the absolute maximum at $\Delta y = \ln(3+\sqrt{8}) \approx 1.76$ and at $\chi = 3$ for the angular distribution in the dijet variable χ.

These features will be considered below in more detail. In order to have more practical analysis, it is convenient to use equidistant binning in $\log\chi$ [36], which corresponds to periodic cell granularity of the calorimeter in η. In this case the smooth χ-spectra (see eqs. (21) and (24)) are transformed into histograms with the maximum in the lowest bin for the gauge bosons with the minimal coupling and with the maximum in the bin containing the value $\chi = 3+\sqrt{8} \approx 5.8$ for the excited bosons (Fig. 12).

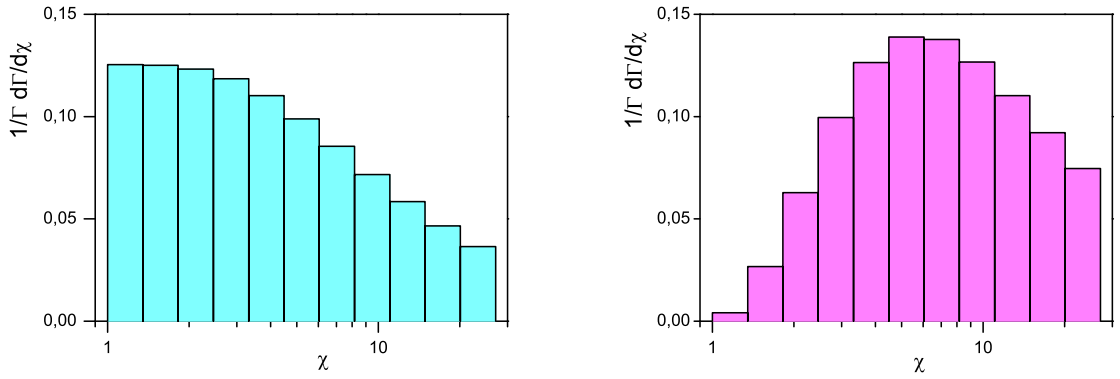

FIG. 12: The normalized histograms of χ-spectra for the gauge bosons with the minimal coupling (left) and for the excited bosons (right). From [18].

Using distributions in (pseudo)rapidity and χ one can construct two useful ratios of numbers of events N measured under specified experimental constraints schematically given below in brackets. The first is the wide-angle to small-angle ratio

$$R_\chi(a,b) = \frac{N(1<\chi<a)}{N(a<\chi<b)} \tag{25}$$

and the second is centrality or the η-ratio of both jets

$$R_\eta(a,b) = \frac{N(|\eta_{1,2}|<a)}{N(a<|\eta_{1,2}|<b)}. \tag{26}$$

The ratios are less affected by the systematic uncertainties and can be used for searching for new physics in dijet data. To understand how they work, let us suppose that one has found some bump in the experimental dijet invariant mass distribution. Then we can compare the angular distributions for "on-peak" events (or events comprising the bump) and "off-peak" events (or events far away from the bump), using the aforementioned ratios. At the moment we ignore the complications of experimental separation of "on-peak" events from the "off-peak" ones. Since the QCD background is dominated by the Rutherford-like distribution, we can consider, as an approximation, a simple case where the QCD dijet χ-distribution is flat. It means that for the selected equal kinematical regions $b - a = a - 1$ ($b = 2a - 1$), the ratio R_χ for the "off-peak" events should be approximately one and does not depend on the dijet mass. When the "on-peak" events originate from the new physics and have the angular distribution different from the one predicted in QCD, the ratio R_χ should deviate from one. Due to an excess at small χ values irrespectiveof the maximal χ-value (in our case equals to a) one has $R_\chi > 1$ for all known exotic models, except the excited bosons, when one expects $R_\chi < 1$.

In order to emphasize the effect of the excited bosons (to increase sensitivity to these bosons), we need to choose a value of a, which makes the ratio as small as possible

$$R_\chi(a, 2a-1) = \frac{N_{\rm QCD} + N_{\rm new}(< a)}{N_{\rm QCD} + N_{\rm new}(> a)} \approx 1 + \frac{N_{\rm new}(< a) - N_{\rm new}(> a)}{N_{\rm QCD}} < 1. \qquad (27)$$

Here $N_{\rm new}(< a)$ and $N_{\rm new}(> a)$ denotes the number of events generated by the new physics in the regions $1 < \chi < a$ and $a < \chi < 2a - 1$, respectively. Simple integration gives the QCD contribution $N_{\rm QCD}(1 < \chi < a) \propto \int_1^a d\chi = N_{\rm QCD}(a < \chi < 2a - 1) \propto \int_a^{2a-1} d\chi = (a-1)$. Simialr integrations of the χ-distribution (24) in $1 < \chi < a$ and $a < \chi < 2a-1$ give $N_{\rm new}(< a) \propto (a-1)^3/(a+1)^3$ and $N_{\rm new}(> a) \propto (a-1)^3/a^3 - N_{\rm new}(< a)$, respectively. Therefore, due to the monotonic increase of the distribution (24) to the maximum at $\chi = 3$ it is possible to reach the minimal value for (27) with the parameters $a \approx 1.87$ and $b \approx 2.74$. In our "ideal" case these parameters are optimal for the search for excited bosons with the ratio (25). The larger value $a \geq 1/(\sqrt[3]{2} - 1) \approx 3.85$ will lead to a compensation of the contributions from the low and high χ-parts ($N_{\rm new}(< a) \approx N_{\rm new}(> a)$), and $R_\chi \geq 1$ again.

For the QCD generated dijets the centrality ratio R_η (26) is also almost constant and should not depend on the dijet invariant mass when the parameters a and b are fixed. When a dijet new-physics signal takes place, this ratio could deviate from its constant value. Signal events for almost all exotic models are expected in the central (pseudo)rapidity region. Therefore, one could see a bump in the R_η distribution as a function of the dijet mass. Contrariwise, the signal from the excited bosons could lead to a novel signature: instead of the bump one will have a dip in the distribution at the resonance mass.

To investigate quantitatively this possibility we have again used the CompHEP package [20, 21], which was extended with the excited bosons model of [37]. In particular, two dimensional pseudorapidity distributions were generated for " $2 \to 2$ " processes proceeding through the gauge W' and excited W^* boson resonances with the same mass 550 GeV/c^2 at $\sqrt{s} = 7$ TeV pp collider (Fig. 13). The CTEQ6L parton distribution functions were used. For both final jets we impose cuts on the pseudorapidity $|\eta| < 2.5$ and the transverse momentum $p_{\rm T} > 30$ GeV/c. To minimize the potential differences in jet response

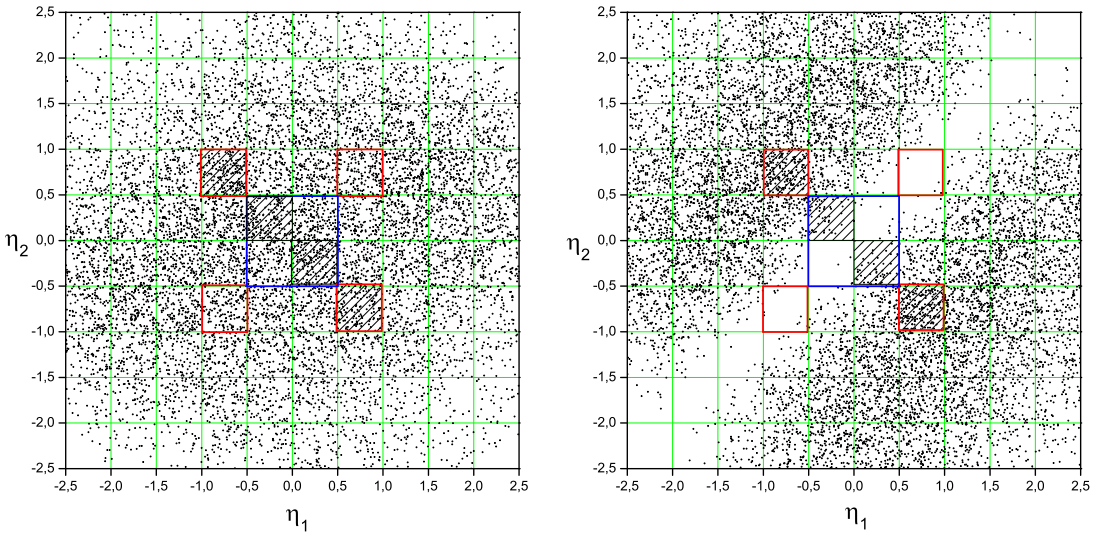

FIG. 13: The two dimensional pseudorapidity distributions (scatter plots) of dijet events for the gauge bosons with the minimal coupling (left) and for the excited bosons (right). The central region $|\eta_{1,2}| < 0.5$ and outer regions $0.5 < |\eta_{1,2}| < 1.0$ are depicted. The hatched squared regions correspond to selected events with opposite pseudorapidity signs. From [18].

and efficiency of jet registration between the *inner* and *outer* dijet events one can choose the central region of the calorimeter $|\eta| < 1$. Using calculations given in the scatter plots (Fig. 13) one can estimate the centrality ratios (26) for the gauge and excited bosons

$$R'_\eta(0.5, 1.0) \simeq 1.08 \qquad \text{and} \qquad R^*_\eta(0.5, 1.0) \simeq 0.29. \tag{28}$$

The dramatic difference between these two numbers is clearly seen, it should lead to the corresponding experimental signature. Since the QCD ratio $R^{\rm QCD}_\eta(0.5, 1.0) \simeq 0.6$ is located *right between* the numbers, the gauge bosons with the minimal coupling will lead to an increase in the QCD ratio at the resonance mass, while the excited bosons should decrease the ratio. It is interesting to notice that a hint of this type of the novel signature can be seen in the low-statistics distribution of the η-ratio versus the dijet invariant mass in the ATLAS data in approximately the same mass range, 450 GeV $< M_{jj} <$ 600 GeV, as for the resonance bump in the dijet events [38].

Unfortunately, one should stress that the extensions of the "signal region" up to $|\eta| < 1.3$ and the central region up to $|\eta| < 0.7$ do not change drastically the QCD ratio $R_\eta^{\rm QCD}(0.7, 1.3) \simeq 0.55$, but dilute the signal from the excited bosons since $R_\eta^*(0.7, 1.3) \simeq 0.68$. In order to increase the sensitivity to the excited bosons one can consider the centrality ratio only for the dijet events with the opposite pseudorapidities $R_\eta|_{(\eta_1\cdot\eta_2)\le 0} = \mathcal{R}_\eta$ (the hatched regions in Fig. 13). In this case the difference between $\mathcal{R}'$ and $\mathcal{R}^*$ increases

$$\mathcal{R}'_\eta(0.5, 1.0) \simeq 1.12 \qquad \text{and} \qquad \mathcal{R}^*_\eta(0.5, 1.0) \simeq 0.25, \tag{29}$$

but we lose half of the statistics. Therefore, it is convenient to consider the distribution in $\Delta\eta \equiv |\eta_1 - \eta_2| \ge 0$ for the events in the rectangle region $\Delta\eta < b$ and $\eta_B \equiv |\eta_1 + \eta_2| < c$. The cut $\eta_B < c$ is necessary to reduce the effect of the parton distribution functions on different $\Delta\eta$ bins. The corresponding centrality ratio $R_{\Delta\eta}$ is defined as

$$R_{\Delta\eta}(a, b, c) = \left.\frac{N(\Delta\eta < a)}{N(a < \Delta\eta < b)}\right|_{\eta_B < c}. \tag{30}$$

The normalized histograms of the $\Delta\eta$-spectra and the theoretical curves are shown in Fig. 14 for the following parameters values: $b = 3.5$ and $c = 1.5$. It can be seen from the

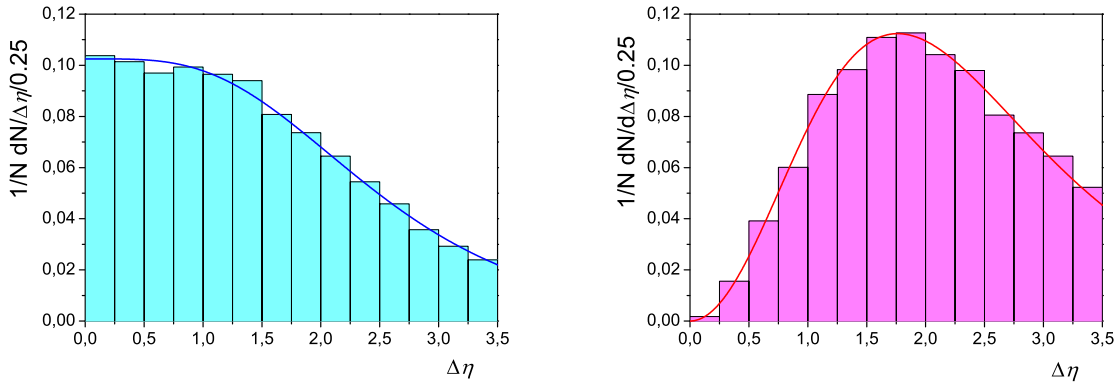

FIG. 14: The normalized histograms of the $\Delta\eta$-spectra for the gauge bosons with the minimal coupling (left) and for the excited bosons (right). The solid curves correspond to the theoretical formulas (21) and (24). From [18].

figure that the theoretical distributions describe very well the above-mentioned simulation data. In the same way as was done for the χ-distribution of the excited bosons one can maximize the deviation of $R_{\Delta\eta}(a, b, c)$ from the QCD ratio $R_{\Delta\eta}^{\rm QCD} = N_{\rm QCD}^{(a)}/N_{\rm QCD}^{(b-a)}$. One finds the desired minimum of $R_{\Delta\eta}(a, b, c)$, which corresponds to the maximal deviation from QCD, for $c = 1.5$, $b = 1$ and $a = 0.67$ [18].

VI. CONCLUSION

In this review phenomenological consequences of the Standard Model extension by means of new spin-1 chiral fields with the internal quantum numbers of the electroweak Higgs doublets are summarized. It is worth stressing that the new type of spin-1 chiral bosons can exist. They are well motivated from the point of view of the Hierarchy problem and are predicted by at least three different classes of theories that represent different approaches to explanation of the relative lightness of the Higgs doublets. The decay distributions of the chiral bosons differ drastically from the distributions of the known gauge bosons and can be distinguished from others. The discovery of this type of distributions will point to existence of compositeness, new symmetry and even extra dimensions.

The prospects for resonance production and detection of the chiral vector Z^* and $W^{*\pm}$ bosons at the LHC energies are considered on the basis of quantitative simulations within the CompHEP/CalcHEP package. The experimental signatures of the excited chiral heavy Z^* bosons are considered and compared with those of the gauge Z' bosons.

The Z^* boson can be observed as a Breit-Wigner resonance peak in the invariant dilepton mass distributions in the same way as the well-known extra gauge Z' bosons. This naturally puts the chiral bosons on the list of very interesting objects for early searches with the first LHC data. Moreover, Z^* bosons have unique signatures in transverse momentum, angular and pseudorapidity distributions of the final decay products, which allow one to distinguish them from other heavy neutral resonances. In particular, there is no Jacobian peak in the transverse momentum distribution of the decay products, and the angular distribution (in the Collins-Soper frame for high on-peak invariant masses) has a peculiar "swallowtail" shape.

In 2010, with 40 pb^{-1} of the LHC proton-proton data at energy 7 TeV, the ATLAS detector was used to search for narrow resonances in the invariant mass spectrum of e^+e^- and $\mu^+\mu^-$ final states and high-mass charged states decaying to a charged lepton and a neutrino. No statistically significant excess above the Standard Model expectation was observed. Therefore, low mass limits of 1.15 TeV/c^2 and 1.35 TeV/c^2 were obtained for the neutral chiral Z^* and charged W^* bosons, respectively. These are the first direct limits on the W^* and Z^* boson production.

Finally, a novel strategy for the neutral chiral boson search in the LHC dijet data is discussed. For almost all currently considered exotic models the relevant signal is expected in the central dijet rapidity region $y_{1,2} \simeq 0$ and $|y_1 - y_2| \simeq 0$. Contrariwise, the excited bosons do not contribute to this region but produce an excess of dijet events far away from it. In particular, for these bosons the appropriate kinematic restrictions can lead to a dip in the centrality ratio distribution over the dijet invariant mass instead of a bump expected in the most exotic models.

We expect that the experimental results, presented here and based on low statistics

of 2010 will be very soon improved with much higher statistics of 2011. Furthermore, we plan to extend our search for excited bosons by means of thorough investigation of the dijet data from the ATLAS detector at the LHC.

Acknowledgments

We are very grateful to O. Fedin and his colleagues for fruitful cooperation, V.G. Kadyshevsky and N.A. Russakovich for support and interest in this research. The work of M.V. Chizhov was partially supported by the grant of the Plenipotentiary of the Republic of Bulgaria in JINR for the year 2011.

---

[1] *Chizhov M. V. //* hep-ph/9610220.

[2] *Ball P. and Braun V. M. //* Phys. Rev. 1996. V.D54. P.2182–2193, hep-ph/9602323.

[3] *Braun V. M. et al. //* Phys. Rev. 2003. V.D68. P.054501, hep-lat/0306006.

[4] *Becirevic D., Lubicz V., Mescia F., and Tarantino C. //* JHEP 2003. V.05. P.007, hep-lat/0301020.

[5] *Chizhov M. V. //* JETP Lett. 2004. V.80. P.73–77, hep-ph/0307100.

[6] *Kemmer N. //* Proc. Roy. Soc. Lond. 1938. V.A166. P.127.

[7] Salam A., (Ed.) and Sezgin E., (Ed.) // , "SUPERGRAVITIES IN DIVERSE DIMENSIONS. VOL. 1, 2." Amsterdam, Netherlands: North-Holland 1499 p., 1989.

[8] *Barate R. et al. //* Eur. Phys. J. 1998. V.C4. P.571–590.

[9] *Abbiendi G. et al. //* Phys. Lett. 2002. V.B544. P.57–72, hep-ex/0206061.

[10] *Achard P. et al. //* Phys. Lett. 2003. V.B568. P.23–34, hep-ex/0306016.

[11] *Adloff C. et al. //* Phys. Lett. 2002. V.B548. P.35–44, hep-ex/0207038.

[12] *Chekanov S. et al. //* Phys. Lett. 2002. V.B549. P.32–47, hep-ex/0109018.

[13] *Acosta D. et al. //* Phys. Rev. Lett. 2005. V.94. P.101802, hep-ex/0410013.

[14] *Abazov V. M. et al. //* Phys. Rev. 2008. V.D77. P.091102, hep-ex/0801.0877.

[15] *Chizhov M. V., Bednyakov V. A., and Budagov J. A. //* Phys. Atom. Nucl. 2008. V.71. P.2096–2100, hep-ph/0801.4235.

[16] *Chizhov M. V. //* hep-ph/0807.5087.

[17] *Chizhov M. V., Bednyakov V. A., and Budagov J. A. //* hep-ph/1005.2728.

[18] *Chizhov M. V., Bednyakov V. A., and Budagov J. A. //* hep-ph/1010.2648.

[19] *Chizhov M. V., Bednyakov V. A., and Budagov J. A. //* hep-ph/1106.4161.

[20] *Pukhov A. et al. //* hep-ph/9908288.

[21] *Boos E. et al. //* Nucl. Instrum. Meth. 2004. V.A534. P.250–259, hep-ph/0403113.

[22] *Pukhov A. //* hep-ph/0412191.

[23] *Chizhov M. V. and Dvali G. //* hep-ph/0908.0924.

[24] Barger V. D. and Phillips R. J. N. // , "COLLIDER PHYSICS." REDWOOD CITY, USA: ADDISON-WESLEY (1987) 592 P. (FRONTIERS IN PHYSICS, 71), 1987.

[25] *Chizhov M. V. //* hep-ph/0609141.

[26] *Chizhov M. V. //* hep-ph/0008187.

[27] *Collins J. C. and Soper D. E. //* Phys. Rev. 1977. V.D16. P.2219.

[28] *Gounaris G., Layssac J., Moultaka G., and Renard F. M. //* Int. J. Mod. Phys. 1993. V.A8. P.3285–3320.

[29] *Aad G. et al. //* JINST 2008. V.3. P.S08003.

[30] *Aad G. et al. //* JHEP 2010. V.09. P.056, hep-ph/1005.5254.

[31] *Aad G. et al. //* Eur. Phys. J. 2011. V.C71. P.1630, hep-ph/1101.2185.

[32] *Aad G. et al. //* Phys. Lett. 2011. V.B700. P.163–180, hep-ph/1103.6218.

[33] *Aad G. et al. //* Phys. Lett. 2011. V.B701. P.50–69, hep-ph/1103.1391.

[34] *Haber H. E. //* hep-ph/9405376.

[35] *Barger V. D., Martin A. D., and Phillips R. J. N. //* Z. Phys. 1983. V.C21. P.99.

[36] *Aad G. et al. //* Phys. Lett. 2011. V.B694. P.327–345, hep-ph/1009.5069.

[37] *Chizhov M. V. //* hep-ph/1005.4287.

[38] *Aad G. et al. //* Phys. Rev. Lett. 2010. V.105. P.161801, hep-ph/1008.2461.